Extraction optimization and bioactivity evaluation of fucoidan from brown seaweed (*Turbinaria conoides*)

Prathapavarma Digala[1,2], Shaik Ibrahim Khalivulla[3]*, Savaraiar Vincent[2,4]*, Palamai Dinakaran[5], Arifullah Mohammed[6], and Mohammad Khairul Azhar Abdul Razab[7]*

ABSTRACT

Brown seaweeds (*Turbinaria conoides*) are marine algae known for producing fucoidan, a sulfated polysaccharide composed of L-fucose monomers. In this study, fucoidan was extracted from *T. conoides* by using a combination of response surface methodology and Box–Behnken design to refine the extraction conditions. The identity of the extracted fucoidan was confirmed by Fourier transform-infrared spectroscopy. 1,1-diphenyl-2-picrylhydrazyl assay demonstrated its antioxidant properties. It also exhibited strong anticancer activity against HeLa cervical cancer cells, while the viability of normal L6 cells remained largely unaffected. Furthermore, acridine orange/ethidium bromide double staining for apoptosis in treated HeLa cells and reactive oxygen species detection using carboxy-2',7'-dichlorodihydrofluorescein diacetate staining confirmed elevated oxidative stress levels induced by fucoidan. These results suggest its ability to both induce and reduce oxidative stress, depending on cell types. Notably, this study is the first to investigate the anticancer effects of fucoidan extracted from *T. conoides* on cervical cancer cells, thus providing a foundational step for future therapeutic development. These findings position *T. conoides*-derived fucoidan as a promising dual-action compound with antioxidant and anticancer capabilities.

Keywords:
Brown seaweed; *Turbinaria conoides*; Fucoidan extraction; Box–Behnken design-response surface methodology; 1,1-diphenyl-2-picrylhydrazyl free radical scavenging; Cervical cancer activity; Apoptosis

***Corresponding authors:**
Shaik Ibrahim Khalivulla, shaik.ibrahim@mbu.asia;
Savaraiar Vincent, svincentloyola@gmail.com;
Mohammad Khairul Azhar Abdul Razab, khairul.azhar@usm.my

How to cite this article:
Digala, P.; Khalivulla, S.I.; Vincent, S.; Dinakaran, P.; Mohammed, A.; Razab, M.K.A.A. Extraction optimization and bioactivity evaluation of fucoidan from brown seaweed (*Turbinaria conoides*). *Biomater Transl.* 2025.

doi: 10.12336/bmt.25.00074

1. Introduction

As a leading cause of global mortality, cancer comprises a diverse group of diseases with distinct etiologies. Among them, cervical cancer is primarily caused by persistent infection with high-risk human papillomavirus (HPV). Specifically, HPV-16 and HPV-18 are implicated in roughly 70% of global cases.[1] According to the National Cancer Registry Programme of India, the age-standardized incidence rate of cervical cancer is estimated to be around 22.4/100,000 women, with regional variations, and higher incidence reported in rural and underserved areas of northern and southern India.[2] It is the second most prevalent cancer among women in the country, with approximately 122,000 new cases and 67,000 deaths reported each year.[3] In India, a significantly high percentage of women have been reported infected with HPV, with studies reporting ranges of 15–25%.[4] Cervical cancer risk factors include early initiation of sexual activity, having multiple sex partners, smoking, inadequate hygiene, and a weakened immune system. Social factors, such as early marriage and multiple childbirths, which are common in rural areas, also significantly contribute to the high incidence of cervical cancer in these regions.[2] Although cervical cancer is a highly preventable disease through vaccination and screening, awareness and access to these interventions are limited in rural India.[1]

Seaweeds are macroscopic marine algae found in oceans and estuaries, particularly in the intertidal zone and shallow subtidal zone. Seaweeds are classified into three main groups: Brown, green, and red algae. All of these are remarkable sources of bioactive compounds, functioning as natural chemical factories. Unlike primary metabolites used for growth, secondary metabolites exhibit a vast array of biological activities.[5] One of the most valuable bioactive compounds found in brown seaweeds is fucoidan, a sulfated L-fucose polysaccharide. However, fucoidan is not a single uniform molecule; its structure can vary depending on the specific seaweed species.[6,7] This structural diversity opens doors for exciting possibilities. Each unique fucoidan extracted from seaweed has the potential to be a novel biomolecule with a distinct structure and potentially unique biological functions. Over the past few years, studies have shed light on the potential of fucoidan and its associated biomolecules as natural therapeutic agents in the medical field.[8] Fucoidan has shown various biological properties, including growth factor trapping and function promotion, neovascularization (new blood vessel formation), fibrillar collagen matrix formation (essential for wound healing), antimicrobial, antioxidant, antiviral, anti-inflammatory, antitumor, anticoagulant activities, and immunostimulatory properties.[9,10] The structure–activity relationship of fucoidan, due to its vast potential, as well as seasonal and geographic differences, remains under investigation.[11] The significant differences in polysaccharides derived from various seaweeds make them highly valuable across various industries, including food, cosmetics, and pharmaceuticals.[6]

Enzymatic extraction techniques, especially those combining cellulases and alginate lyases, significantly improve fucoidan yields compared to chemical methods, achieving fucose recovery rates of up to 87% in *Saccharina latissima* and 78% in *Alaria esculenta*. Moreover, the fucoidans obtained through these enzymatic methods exhibit high sulfate content, ranging from 45–47% and 40–45% of the dry matter for the respective species.[12] In contrast, the present study optimized the extraction of fucoidan from *Turbinaria conoides* under acidic conditions. This study delves into exciting possibilities by employing response surface methodology (RSM) with a focus on the Box–Behnken design (BBD) to optimize fucoidan extraction from *T. conoides* seaweed. This optimization involved analyzing various factors, including temperature, pH, time, and algal ratio, that influence fucoidan yield. Modern research frequently employs RSM as an effective tool for optimizing processes, involving multiple variables, offering accurate results with fewer experiments and reduced time.[13,14]

Evaluating the ability of the extracted fucoidan to act as an antioxidant provided valuable insights into its ability to combat free radicals. Human bodies naturally produce reactive oxygen species (ROS) as byproducts of various cellular metabolic processes. Low levels of ROS trigger signaling pathways that initiate biological processes, whereas oxidative stress, caused by high ROS levels, can disturb the redox balance and damage lipids, proteins, and DNA. This damage may lead to cell injury and contribute to the development of various diseases, including neurodegenerative disorders, cancer, respiratory, cardiovascular, and digestive diseases.[15,16] The extracted fucoidan demonstrates strong antioxidant properties, laying the groundwork for additional research exploring its potential therapeutic applications. Subsequently, *T. conoides* has been reported as a potential natural antioxidant.[17-19]

The ability to induce apoptosis and programmed cell death is one of fucoidan's most crucial anticancer properties. Fucoidan can initiate various apoptotic pathways. These include both the internal mitochondrial pathway and the external death receptor pathway. It has been shown to increase levels of pro-apoptotic proteins, such as BAX, while decreasing anti-apoptotic proteins, such as BCL-2, resulting in mitochondrial dysfunction and the activation of caspases that trigger cell death.[20] Furthermore, fucoidan has been shown to upregulate the expression of death receptor ligands, such as FASL (CD95L/Apo1L), which activates the extrinsic apoptotic pathway in specific cancer cell types.[21] Fucoidan has been shown to induce cell cycle arrest in various cancer cell types, specifically at the G0/G1 and G2/M checkpoints. This results in the cessation of cancer cell division and, therefore, tumor growth. It has been shown that fucoidan blocks cyclins (such as cyclin D1 and cyclin B1) and cyclin-dependent kinase, which are crucial for the cell cycle to progress.[22] By blocking these regulators, fucoidan prevents cancer cells from proceeding with the cell cycle and entering mitosis. Fucoidan has also been reported to have anti-metastatic effects. It suppresses the activity of matrix metalloproteinases (MMPs), enzymes that break down the extracellular matrix and facilitate metastasis. By reducing MMP activity, fucoidan hinders the cancer cells' ability to infiltrate surrounding tissues and spread to distant organs.[23]

Angiogenesis—the growth of new blood vessels—is the most important factor for tumor progression and metastasis. Fucoidan downregulates numerous signaling pathways involved in the development of new blood vessels, such as vascular endothelial growth factor (VEGF), thereby depriving tumor cells of basic nutrients and oxygen, and halting tumor growth and proliferation.[24] The immunomodulatory effects of fucoidan enhance the body's immune response by boosting the activity of immune cells, such as macrophages, dendritic cells, and natural killer cells, in the recognition and destruction of cancer cells. Moreover, fucoidan elevates cytokine production, including interleukins (ILs), such as IL-1 and IL-6, thereby

[1]Department of Medical Laboratory Technology, School of Medical Health and Allied Sciences, MNR University, Fasalwadi, Sangareddy, Telangana, India; [2]Environnex Innovation and Research Foundation, Chennai, Tamil Nadu, India; [3]Department of Biological and Chemical Sciences, Faculty of Liberal Arts and Sciences, Mohan Babu University, Tirupati, Andhra Pradesh, India; [4]Centre for Environmental Research and Development, Loyola Institute of Frontier Energy, Loyola College, Chennai, Tamil Nadu, India; [5]Jen Multi-Speciality Clinic, Chennai, Tamil Nadu, India; [6]Department of Biotechnology, Koneru Lakshmaiah University, Vaddeswaram Campus, Guntur, Andhra Pradesh, India; [7]Department of Radiation, School of Health Sciences, Universiti Sains Malaysia, Health Campus, Kubang Kerian, Kelantan, Malaysia

enhancing the antitumor immune response.[25] Fucoidan has been shown to modulate the nuclear factor kappa-light-chain-enhancer of activated B cells (NF-κB) signaling pathway, which is frequently overactivated in cancer cells and contributes to tumor development, inflammation, and resistance to apoptosis. This pathway supports cancer cell survival, growth, and metastasis. By suppressing NF-κB activation, fucoidan reduces the expression of genes that promote these cancerous behaviors. This makes fucoidan an effective agent in targeting molecular pathways that support tumor growth.[26] Fucoidan exerts anticancer activities through multiple modulatory roles in critical tumorigenesis pathways, including the initiation of apoptosis and cell cycle arrest, as well as effects on metastasis, angiogenesis, immune system modulation, and oxidative stress. These mechanisms make this compound a promising chemopreventive and therapeutic agent for cancer, although its effects have been demonstrated only in earlier pre-clinical studies.

Therefore, the present study aimed to evaluate the effects of various factors, including temperature, pH, extraction time, and water-to-seaweed ratio, on fucoidan yield from *T. conoides* using BBD-RSM. The structure of fucoidan was confirmed by Fourier transform infrared spectroscopy (FTIR), and its pharmacological properties, including antioxidant activity, cytotoxicity against HeLa (cervical cancer cell line), and apoptotic features, were assessed using the acridine orange (AO) and ethidium bromide (EB) double-staining technique.

2. Materials and methods

2.1. Seaweed sample collection

The brown seaweed *T. conoides* was carefully collected from a specific location at Mandapam, located in the Gulf of Mannar at latitude 09°17'N and longitude 79°08'E, near Rameshwaram, Tamil Nadu, India. The *T. conoides* was first washed thoroughly in seawater to remove any unwanted debris or surface contaminants, then rinsed with distilled water. This additional cleaning step ensured the removal of any residual salts or impurities that might have remained after the seawater wash before shade drying at room temperature. Shade drying prevented excessive heat from degrading seaweed compounds. Finally, the dried seaweed was chopped into smaller pieces and subsequently ground into a fine powder using a mixer grinder.

2.2. Extraction of fucoidan

A modified version of the fucoidan extraction method described by Suresh *et al.*[27] was employed. To eliminate unwanted lipids, proteins, and pigments, 100 g of *T. conoides* powder was treated with 1 L of ethanol. The mixture was stirred using a mechanical stirrer for about 12 h at room temperature, then centrifuged at 3,000 rpm for 10 min. The resulting residue was subsequently dried at room temperature. About 5 g of the residue or defatted seaweed biomass was treated with 100 mL of 0.01 M HCl (pH 2.0), 0.1 M sodium hydroxide (pH 13.0), and distilled water (pH 7.0) for acidic, basic, and neutral medium samples, respectively, at a high temperature of 90°C for 3 h under constant stirring. The extraction was repeated three times to maximize fucoidan yield, and the resulting extracts were combined. The pooled extracts were centrifuged at a high speed (15,000 rpm) for 10 min to remove any remaining solid particles. The clear supernatant, containing the extracted fucoidan, was carefully collected for further processing. This supernatant may also contain another major polysaccharide, alginic acid. About 1% of calcium chloride ($CaCl_2$) solution was mixed with the fucoidan-containing supernatant, and the mixture was kept at a cold temperature (4°C) for 12 h to allow alginic acid to precipitate. The solution was subsequently centrifuged at 15,000 rpm for 10 min to separate the precipitated alginic acid from the fucoidan-rich supernatant. Ethanol (99%) was then added gradually to the supernatant in a controlled manner, first reaching a final concentration of 30% and then 70%. After each ethanol addition, the solution was kept at 4°C for a specified time (4 h for 30% ethanol and overnight for 70% ethanol). Centrifugation at 15,000 rpm for 10 min was performed after each ethanol treatment, allowing for the collection of the fucoidan-enriched pellet.

2.3. RSM

RSM is a statistical technique developed to optimize complex processes, such as the extraction of bioactive polysaccharide compounds. It offers the advantage of minimizing the number of experimental trials required to assess multiple parameters and their interactions.[28] Furthermore, BBD is a widely used approach in RSM.[29] In this study, RSM incorporating a BBD with four factors at three levels was employed to optimize the extraction of polysaccharides from *T. coinoides*. The BBD was selected to evaluate and optimize the effects of key process variables extraction temperature (60, 80, and 100°C), pH (3, 5, and 7), extraction time (1, 3, and 5 h), and buffer-to-algal ratio (1:10, 1:40, and 1:60 g/mL) on the crude yield and properties of the extracted fucoidan.

2.4. BBD-RSM experimental design

A systematic BBD-RSM was employed to assess the influence of acidic extraction process variables on the yield of fucoidan extracted from *T. coinoides*. The Box-Behnken statistical design was utilized to optimize extraction parameters and evaluate the significant interactive effects among them on fucoidan yield.[30] RSM was further applied to derive multivariate equations representing these relationships. An orthogonal array of 24 BBD experimental runs, including five replicates at the center points, each performed in duplicate, resulted in a total of 29 experiments designed to optimize key variables in the acidic extraction of fucoidan. The center points were included to estimate pure error and detect any curvature in the response. The interactions among variables and their optimal levels were described using a second-order polynomial equation. A generalized version of this equation, using coded process parameters, was formulated (Equation [1]).

$$x_i = \frac{x_{i-x_0}}{\Delta x} \quad (1)$$

Here, the coded value X_i represents the i variable, while X_i (uncoded) denotes the actual value of the independent variable (i), and X_o is the uncoded value of the i variable at the center

point. The percentage of polysaccharides extracted serves as the response variable. A regression analysis was conducted to model the response using a second-order polynomial (Equation [2]).

$$Y = \beta_0 + \sum_{i=1}^{k} \beta_i X_i^2 + \sum_{i=1}^{k} \beta_{ii} X_{ii}^2 + \sum_{i=1}^{k-1} \sum_{j=2}^{k} \beta_{ij} X_i X_j \quad (2)$$

where Y denotes the predicted response, and o, i, ii, and ij represent the regression coefficients.[29] These correspond to the constant term, as well as the linear, quadratic, and interaction effects of the X_1–X_3 factor responses, respectively. The regression analysis and coefficient estimation were performed using Design Expert software (Trial version 7.1.5, Stat-Ease Inc., USA). The resulting equations were statistically validated through analysis of variance (ANOVA). The significance of each term in the equation was assessed to determine the model's goodness of fit. Optimal values for the test variables were initially identified in coded units and subsequently converted to actual (uncoded) units.

2.5. FTIR

Approximately 2 mg of acidic, basic, and neutral fucoidan samples were separately ground with 100 mg of potassium bromide (KBr) and prepared as pellets. The FTIR spectrum was recorded for each KBr pellet.

2.6. 1,1-Diphenyl-2-picrylhydrazyl assay

To evaluate the antioxidant activity of the extracted fucoidan, the 1,1-diphenyl-2-picrylhydrazyl (DPPH) radical scavenging assay was employed, following the method described by Liyana-Pathirana and Shahidi.[31] A 0.135 mM DPPH solution was prepared in methanol. Fucoidan extract solutions of varying concentrations (ranging from 0.02 mg/mL to 0.1 mg/mL) were also prepared in methanol. Equal volumes (1.0 mL) of each fucoidan concentration and the DPPH solution were combined, allowing interaction between the DPPH free radicals and potential antioxidants in the extract. The mixtures were thoroughly vortexed and incubated at room temperature (27°C) in the dark for 30 min to prevent light-induced degradation of DPPH. After incubation, the absorbance of each mixture was measured at 517 nm using a spectrophotometer, enabling quantification of the remaining DPPH radicals. Butylated hydroxytoluene, a known synthetic antioxidant, was used as a reference standard. The DPPH radical scavenging activity of the fucoidan extract was then calculated using Equation (3).

$$\text{DPPH radical scavenging activity}(\%) = \frac{\text{Absorbance of control} - \text{Absorbance of sample}}{\text{Absorbance of control}} \times 100 \quad (3)$$

This equation considers both the initial absorbance of the DPPH solution and the absorbance of the reaction mixture after incubation with the extract. A higher percentage of DPPH radical scavenging activity reflects a stronger antioxidant potential of the fucoidan extract. The DPPH assay provided valuable insights into the extract's ability to scavenge free radicals, highlighting its potential contribution to overall antioxidant activity.

2.7. Cell culture and maintenance

Normal cells derived from rat skeletal muscle tissue (L6) and human cervical cancer cells (HeLa) were obtained from the National Centre for Cell Sciences, Pune, India. The cells were cultured in Dulbecco's Modified Eagle Medium (DMEM, Himedia, India), enriched with 10% heat-inactivated fetal bovine serum (FBS) and 1% antibiotic mixture comprising penicillin (100 U/mL), streptomycin (100 µg/mL), and amphotericin B (2.5 µg/mL). Cultures were maintained in 25 cm^2 tissue culture flasks and incubated at 37°C in a humidified atmosphere containing 5% carbon dioxide using an incubator (Galaxy® 170, Eppendorf, Germany). For long-term storage, cells at a low passage number were cryopreserved in the vapor phase of liquid nitrogen using modified culture medium supplemented with 20% FBS and 10% dimethyl sulfoxide (DMSO) or glycerol.

2.8. Inverted phase contrast microscopy

After sample addition, the viability of the treated and the control wells was evaluated by direct observation at regular intervals up to 24 h in an inverted phase-contrast tissue culture microscope (TCM-400, Labomed, USA), and the observations were photographed. The viability and quantification of all the cells were further assessed using the methylthiazol tetrazolium (MTT) assay.

2.9. MTT assay

The cytotoxic and anticancer effects of fucoidan were evaluated using the MTT reduction assay, as described by Mosmann,[32] to determine cell viability. Cultured L6 and HeLa cells were seeded into 96-well plates at a final volume of 100 µL per well. After 24 h, the cells were treated with fucoidan at concentrations of 50, 100, 200, 400, and 800 µg. Subsequently, 100 µL of MTT solution (5 mg/mL) was added to each well. Two wells without cells were used as blanks. The plates were incubated at 37°C for 4 h. Following incubation, the supernatant was removed, and 100 µL of DMSO was added to each well to dissolve the formazan crystals. Absorbance was measured at 570 nm using a microplate reader. Morphological changes, such as cell rounding, shrinkage, granulation, and cytoplasmic vacuolization, were considered indicators of cytotoxicity. All experiments were performed in triplicate. Cell viability was calculated using Equation (4).

$$\text{Cell viability}\,\% = \frac{\text{Avareage absorbance of treated cells}}{\text{Average absorbance of control cells}} \times 100 \quad (4)$$

2.10. Dual AO/EB fluorescent staining

HeLa cells were cultured in 6-well plates using DMEM medium supplemented with 10% FBS and 1% antibiotic cocktail. After 2–3 days of incubation, when the cells reached 70–80% confluence, they were treated with 170 µg/mL fucoidan (half-maximal inhibitory concentration [IC_{50}]: 172.69 µg/mL)

and incubated for an additional 24 h. Untreated cells served as the control. Following incubation, the cells were washed with cold phosphate-buffered saline (PBS) and stained at room temperature for 10 min with a mixture of AO and EB, each at 100 μg/mL. The stained cells were then washed twice with 1 × PBS and examined under a fluorescence microscope (CKX41, Olympus, Japan) using a blue filter.

Based on the fluorescence and appearance, the cells were divided into four categories for interpretation. Light green circular nucleus at the center of the cell indicated the normal living cells; bright yellowish green nucleus with condensed or fragmented chromatin, crescent or granular appearance at one side of the cell indicated the early apoptotic cells; orange nucleus with chromatin condensation or fragmentation indicated the late apoptotic cells; and, uneven bright orange red fluorescence with increased cell volume indicated the necrotic cells.

2.11. Detection of ROSs using carboxy-2',7'-dichlorodihydrofluorescein diacetate

Carboxy-2',7'-dichlorodihydrofluorescein diacetate (H_2DCFDA) is a non-fluorescent compound that becomes green fluorescent upon oxidation in the presence of ROS. A fresh stock solution of carboxy-H_2DCFDA was first prepared and dissolved in sterile DMSO or 100% ethanol. The HeLa cells were washed with PBS to eliminate any residual culture medium, then loaded with the dye. Using a final concentration of 100 μM carboxy-H_2DCFDA in standard culture medium supplemented with 2% serum. The cells were incubated for 30 minutes in the dark at 37°C in a 5% CO_2 incubator. After incubation, the medium containing carboxy-H_2DCFDA was removed, and the cells were washed twice with PBS. Fresh medium containing 0.05% hydrogen peroxide (positive control) or ~170 μg/mL fucoidan ($IC_{50;}$ 172.69 μg/mL) was added to the dye-loaded cells, and the cells were incubated for 1 h. The ROS levels were evaluated by promptly analyzing the cells using fluorescence microscopy.

2.12. Statistical analysis

To ensure the reliability of findings, we conducted each experiment three times. This allowed the calculation of the mean value and the standard error of the mean (SEM) for each data point. The SEM provided a measure of variability within the data set. Statistical analysis was subsequently conducted using GraphPad Prism software (v6, Dotmatics, United Kingdom). This process evaluated whether the differences observed between groups are meaningful or likely due to random variation. In this study, a $p<0.05$ was considered statistically significant, indicating that the results were unlikely to occur by chance.

3. Results and discussion

3.1. Extraction of fucoidan

Fucoidan was extracted from *T. conoides* using three extraction methods: Acidic, alkaline, and neutral. The dry weight yield from **Table 1** represented the percentage of the final product (presumably fucoidan-enriched extract) compared to the initial dry weight of the seaweed used. The acidic extract exhibited the highest dry weight yield (55.0 ± 0.4%), suggesting it might be the most efficient extraction method in terms of recovered material. The acidic extract also yielded the highest sugar content (48.1 ± 0.21%), which could be fucose sugar, a key component of fucoidan. However, it may be due to the presence of other sugars besides fucose. The sulfate content indicated that the fucoidan was a sulfated polysaccharide. The sulfate content indicated the degree of sulfation in the extract. While the acidic extract had the highest dry weight yield, the alkaline extract had the highest sulfate content (7.4 ± 0.6%), suggesting a potentially higher fucoidan concentration in that extract.

3.2. Optimization of BBD

From **Table 2**, the temperature factor varied across a coded range of −1 to 1, corresponding to the temperature range of 60°C to 100°C. Similar to temperature, the pH values ranged from −1 to 1, corresponding to an actual pH range of 3 to 7 used in the experiment. The buffer-to-alga ratio, which was crucial for maintaining optimal extraction conditions, was also varied within a coded range of −1 to 1, corresponding to the ratios of 1:10, 1:40, and 1:60, respectively. The duration of the extraction process, −1 to 1, corresponded to a time range of 1–5 h.

Table 3 shows the dry-weight yield of fucoidan extract measured for each run, as calculated by the BBD. These actual values ranged from 12.00% to 55.00%, with an average yield of 36.97% and a standard deviation of 13.49%. This indicates some variability in the amount of fucoidan extracted under different combinations of variables. The RSM model also generated predicted values for fucoidan yield using the chosen mathematical equation and the combination of variables used in each run. These predicted values ranged from 16.08% to 55.00%, with an average of 36.28% and a standard deviation of 12.75%. A close match between an average of actual and predicted values suggested that the RSM model effectively captured the underlying trends in the data. This analysis of the RSM experiment data lays the groundwork for further exploration. The scatter plot shows a generally strong

Table 1. Yield and composition of total polysaccharide from *Turbinaria conoides*

Extract	Dry weight yield (%)	Sugar content (%)	Sulfate content (%)
Acidic extract	55.0±0.40	48.10±0.21	3.50±0.80
Neutral extract	24.5±0.71	9.80±0.30	4.30±0.90
Alkaline extract	38.2±0.33	3.50±0.70	7.40±0.60

Note: Each value is expressed as mean±standard deviation (n=3).

Table 2. The coded and uncoded forms of variables in the extraction of fucoidan

Variables	Range and levels		
	−1	0	+1
Extraction temperature (°C)	60	80	100
Extraction pH	3	5	7
Buffer to algal ratio (g/mL)	1:10	1:40	1:60
Extraction time (hours)	1	3	5

Table 3. Response surface, Box–Behnken (uncoded), and results for the extraction of fucoidan

Run	Temperature (°C)	pH	Buffer: algal ratio	Time	Actual value (%)	Predicted value (%)
1	0	0	0	0	55.00	55.00
2	1	0	1	0	28.00	27.50
3	−1	0	1	0	15.00	26.42
4	1	0	−1	0	12.00	16.58
5	−1	1	0	0	38.00	24.50
6	0	0	0	0	55.00	55.00
7	0	−1	−1	0	21.00	22.25
8	1	−1	0	0	25.00	32.83
9	1	0	0	−1	19.00	16.08
10	0	−1	0	1	26.00	30.42
11	−1	0	0	1	47.00	41.58
12	−1	0	−1	0	27.00	25.25
13	0	0	0	0	55.00	55.00
14	0	0	−1	1	42.00	44.17
15	1	0	0	1	47.00	43.25
16	0	1	0	−1	46.00	47.42
17	0	0	0	0	55.00	55.00
18	0	1	0	1	28.00	17.17
19	0	0	1	1	32.00	21.92
20	−1	0	0	−1	38.00	45.08
21	0	−1	0	0	47.00	41.83
22	0	0	1	−1	20.00	25.08
23	0	−1	1	0	45.00	43.25
24	1	1	0	0	26.00	30.33
25	0	0	0	0	29.00	28.92
26	−1	−1	0	0	48.00	40.67
27	0	0	0	0	49.00	38.42
28	0	0	−1	−1	42.00	46.08
29	0	0	0	0	55.00	55.00

correlation between actual and predicted values, as indicated by the points clustering around the diagonal line (**Figure 1**).

Figure 1 illustrates that the data generated using BBD-RSM provided a good, valid model. Predicted and experimental values were closely aligned along the diagonal line, indicating that the outcome was valid in this design. At the optimum conditions, such as the temperature at 70°C, with a duration of 3 h, an acidic pH of 3, and a buffer to algal ratio of 1:40 g/mL, the obtained experimental yield was 55.0 ± 0.4% which was in close agreement with the predicted yield of 55.00 ± 9.24%, obtained from four independent experiments. This indicated that our design model was valid.

The extraction yield statistics for the chosen quadratic predictive model are shown in **Table 4**. The coefficient of variation was 25.71, and the values for the regression coefficient (R^2) and adjusted coefficient of determination (R_{adj}^2) were found to be 0.5780 and 0.7890, respectively, indicating a high degree of precision and reliability of the experimental values and a high degree of correlation between the observed and predicted values.[29,30]

The ANOVA analysis is shown in **Table 5**. The significance of each coefficient was assessed using *p*-values; a small *p*-value (<0.05) indicated a significant coefficient. The linear coefficient, quadratic term coefficients (A^2, B^2, C^2, D^2), and cross-product coefficients were found to be significant ($p<0.05$). Other term coefficients showed in the design were not significant ($p>0.05$). Equation (2) was used to create three-dimensional and two-dimensional contour plots to predict the connection between the individual and the dependent variables.

3.3. Predicted and experimental values of the responses at optimum conditions

Figure 1 illustrates that the data generated using BBD-RSM fit a good, valid model. Experimental (predicted) and actual values scattered near the diagonal line, indicating that the validity of the outcome was accurate in this design. The optimum extraction conditions were estimated using Equation (1) by fitting the regression equation and analyzing the response surface contour plots. From the fitted Equation (2) under optimal conditions, the predicted yield was 55.00 ± 9.24%, which aligns with the experimentally determined mean of 55.00% from four independent experiments (**Table 6**). These results indicate that our design model is valid.

3.4. FTIR analysis for the characterization of fucoidan

The fucoidan showed FTIR vibrations of acidic-, basic-, and neutral-medium extracts of characteristic sulfate (SO_3^{2-}) groups at 1,030, 1,030, and 1012 cm^{-1}, hydroxyl groups (–OH) at 3,495, 3,542, 3,300 cm^{-1}, and the –CH stretching vibrations at 2,960, 2,965, and 2,986 cm^{-1}, respectively (**Figure 2**).[4,33] The FTIR spectral data confirm the presence of alkyl, sulfate, and hydroxy groups in fucoidan (sulfated polysaccharide) in acidic, basic, and neutral medium-extracted samples.

3.5. Antioxidant activity

The antioxidant activity of fucoidan from *T. conoides* was assessed by using the DPPH assay. At a concentration of 500 μg/mL, fucoidan demonstrated the strongest inhibition (94%) compared to the control (ascorbic acid) (81.05%). In contrast, at 100 μg/mL, it exhibited the weakest inhibition (46%) compared to the control (30.14%) (**Table 7**). The inhibition of DPPH free radical scavenging activity was statistically significant, and the scavenging effect of the fucoidan increased with the amount of sulfate content present in the fucoidan. The DPPH radical is scavenged by an antioxidant through the donation of hydrogen to form a stable DPPH molecule. The DPPH molecule shares similar structural features, such as –OH and $–OSO_3H$ groups. In this case, excess –OH groups were replaced by $–OSO_3H$ groups, contributing to the observed scavenging effect.[18] These findings indicate that the presence of sulfate groups in polysaccharides influences their biological activities.[34] The results of the present study demonstrate that the fucoidan extracted from the *T. conoides* exhibited a significant antioxidant activity. This suggests that the polysaccharide (fucoidan) can be a potential therapeutic agent for cancer treatment.

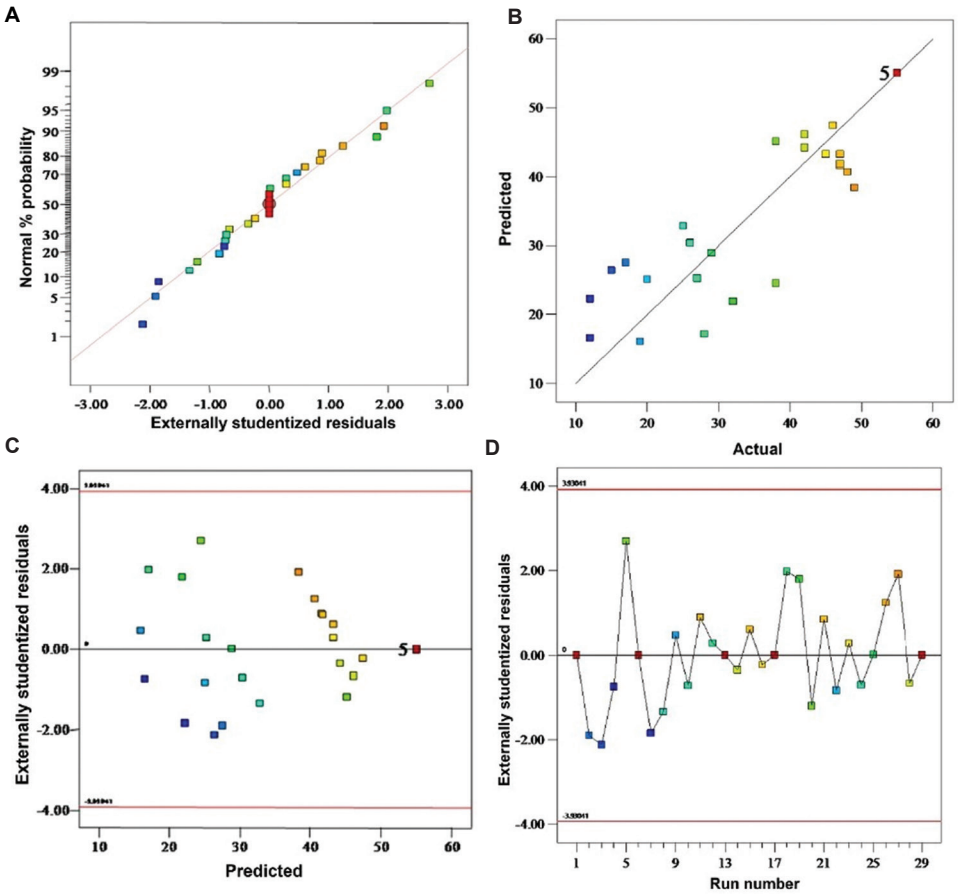

Figure 1. Response surface plots. (A) Normal probability plot of studentized residuals for the extraction of fucoidan. (B) The actual and predicted fucoidan extraction yield. (C) Graph of residuals vs. predicted model. (D) Graph of residual observation order for performance in the fucoidan yield.

Table 4. Analysis of variance for the fitted quadratic polynomial model of the extraction of *Turbinaria conoides*

Source	Sum of squares	Df	Mean square	*F*-value	*p*-value
Model	4,552.29	14	325.16	3.74	0.0095
Residual	1,217.50	14	86.96		
Lack of Fit	1,217.50	10	121.75		
Pure error	0	4	0		
Cor total	5,769.79	28			
	R^2=0.7890	R_{adj}^2=0.5780	CV=25.71		

Abbreviations: CV: Coefficient of variation, Df: Degree of freedom.

Table 5. Analysis of variance for a response surface quadratic model of fucoidan extraction from *Turbinaria conoides*

Source	Sum of squares	Df	Mean square	*F*-value	*p*-value
A (temperature)	507.00	1	507.00	5.83	0.0300
B (pH)	21.33	1	21.33	0.2453	0.6281
C (algal ratio)	21.33	1	21.33	0.2453	0.6281
D (time duration)	0.3333	1	0.3333	0.0038	0.9515
AB	289.00	1	289.00	3.32	0.0897
AC	110.25	1	110.25	1.27	0.2791
AD	12.25	1	12.25	0.1409	0.7131
BC	576.00	1	576.00	6.62	0.0221
BD	289.00	1	289.00	3.32	0.0897
CD	506.25	1	506.25	5.82	0.0301
A^2	1117.40	1	1117.40	12.85	0.0030
B^2	953.61	1	953.61	10.97	0.0051
C^2	876.59	1	876.59	10.08	0.0067
D^2	454.97	1	454.97	5.23	0.0383

Abbreviation: Df: Degree of freedom.

3.6. Anticancer activity

Several studies have assessed the anticancer properties of fucoidan extracted from brown seaweeds against multiple cancer cell lines, suggesting its potential as a cancer treatment. The anticancer activity of fucoidan from *Undaria pinnatifida* was demonstrated by its inhibitory effect against HeLa cells.[35,36] Around 90% of cancer-related deaths were due to metastasis. MMPs play an important role in tumor metastasis. In the present study, a high concentration of fucoidan was found to suppress the expression and secretion of VEGF and MMP-2 in cervical cancer cells. The cells were exposed to fucoidan from 50 to 800 μg/mL for 24 h, the MTT assay was performed, and the microscopic images of cells were captured. To our knowledge, this is the first study to investigate the effects of fucoidan isolated from *T. conoides* on cervical cancer using HeLa cells.

3.6.1. In vitro L6 cell line study

The morphology of L6 cells treated with increasing concentrations of fucoidan (0–800 μg/mL) was examined (**Figure 3**). Across all concentrations, the cells maintained a healthy, well-spread morphology with no significant signs of cytotoxicity or detachment. These observations indicate that fucoidan did not exert adverse morphological effects on L6 cells, even at the highest tested concentration.

In the L6 cell line, fucoidan treatment across a range of concentrations (50–800 μg/mL) resulted in minimal changes in cell viability (**Figure 4**). The control group (0 μg/mL) showed a baseline value of approximately 0.942. At 50 μg/mL, there was a slight decrease, indicating a minimal inhibitory effect at low concentration. However, as the concentration increased to 100, 200, and 400 μg/mL, the sample value increased progressively, with the highest response observed at 400 μg/mL (approximately 0.967), suggesting a dose-dependent enhancement of cellular activity. At 800 μg/mL, the value declined slightly, indicating a potential saturation point or mild cytotoxicity at higher concentrations. Overall, the data suggest that fucoidan promotes cellular activity in L6 cells up to an optimal concentration, beyond which the effect diminishes. Error bars indicate relatively low variability, supporting the reliability of the results.

Table 6. Predicted and experimental values of the responses at optimal conditions

Variables	Value	Experimental yield (%)	Predicted yield (%)
Temperature (°C)	70	55.00	55.00±9.24
Time (h)	3		
pH	5		
Buffer to algal ratio	1:30		

Table 7. 1,1-diphenyl-2-picrylhydrazyl free radical scavenging activity of fucoidan from *Turbinaria conoides*

Concentration (ug/mL)	Inhibition (%)	
	Ascorbic acid (control)	Fucoidan
100	30.14±2.20	46.0±2.38
200	43.67±1.50	50.7±2.19
300	58.12±1.63	67.1±1.70
400	69.11±2.90	78.8±2.20
500	81.05±1.80	94.0±2.20

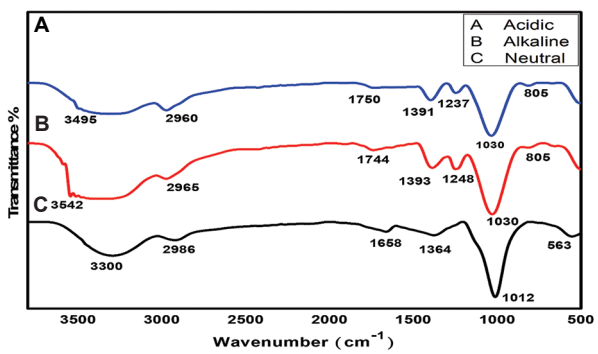

Figure 2. Fourier transform infrared spectroscopy spectra of fucoidan. (A) Acidic extraction. (B) Alkaline extraction. (C) Neutral extraction.

3.6.2. In vitro HeLa cell line study

Figure 5 displays a series of microscopic views of morphological changes in HeLa cells treated with increasing concentrations of fucoidan extracted from *T. conoides*. The panels include a control group (untreated) and cells treated with fucoidan at concentrations of 50, 100, 200, 400, and 800 μg/mL. These images illustrate the dose-dependent cytotoxic effects of fucoidan on the HeLa cells. In the control image, cells appeared healthy and confluent, with normal morphology, intact cell membranes, and tightly packed monolayers. However, as the fucoidan concentration increased, a progressive decline in cell density was observed, accompanied by clear morphological alterations. At 50 and 100 μg/mL, early signs of cytotoxicity were evident, with some cells appearing shrunken or rounded. At 200 and 400 μg/mL, the disruption became more pronounced, and cells lost their adherence, became rounded, and showed signs of detachment. At the highest concentration (800 μg/mL), there was a significant loss of viable cells, with extensive morphological changes, indicating apoptosis or cell death. This pattern supports the conclusion that fucoidan from *T. conoides* exerts a potent anticancer effect against HeLa cells in a dose-dependent manner.

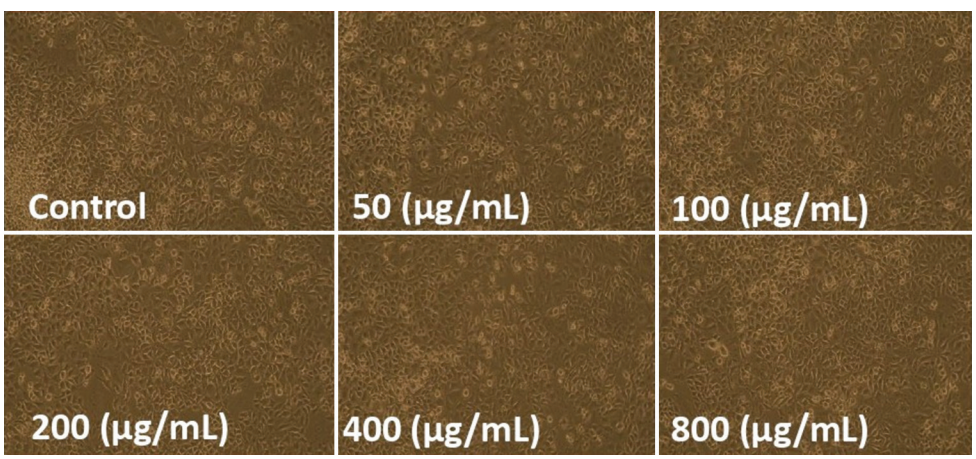

Figure 3. Microscopic images of L6 (normal rat skeletal muscle) cell line treated with different concentrations of fucoidan (0 [Control], 50, 100, 200, 400, 800 μg/mL).

Figure 6 shows a progressive decrease in cell viability with increasing fucoidan concentration, indicating a dose-dependent cytotoxic effect. Specifically, viability declined from 100% in the control group to approximately 45% at 800 µg/mL. Using a four-parameter logistic regression model, the IC_{50} of fucoidan was estimated at 172.69 µg/mL. This value represents the concentration required to reduce cell viability by 50%, suggesting that fucoidan exhibits moderate cytotoxic activity against HeLa cells. This pronounced cytotoxicity against cancerous cells highlights fucoidan's potential as an anticancer agent. Importantly, the stark difference in response between L6 and HeLa cells indicates that fucoidan exhibits selective toxicity in suppressing the growth of cancer cells while leaving normal cells unharmed. Such selectivity is a critical feature for any candidate in cancer therapeutics, as it minimizes damage to healthy tissues during treatment.

3.6.3. Determination of apoptosis by AO and EB double staining

The apoptosis process is characterized by distinct ultrastructural and biochemical changes in cells, including chromatin aggregation, cytoplasmic condensation, and nuclear and cytoplasmic membrane indentation. Apoptotic cells exhibit increased membrane permeability to fluorescent dyes, such as AO and EB, enabling the detection of apoptosis-associated biochemical modifications.[37,38]

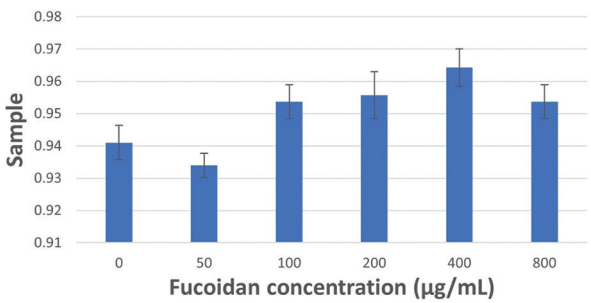

Figure 4. Dose-dependent graph of L6 (normal rat skeletal muscle) cell line treated with different concentrations of fucoidan (0 [Control], 50, 100, 200, 400, 800 µg/mL).

In this study, we evaluated the potential anticancer effects of fucoidan derived from *T. conoides* on cervical cancer cells, specifically HeLa cells, *in vitro*, along with its possible mechanism of action. Using fluorescence microscopy, necrotic and apoptotic cells were distinguished based on overall cell morphology and membrane integrity. Morphological changes were assessed by AO/EB fluorescence staining after treating the cells with fucoidan at its IC_{50} concentration for 24 h. As a result, apoptotic cells exhibited condensed nuclei and orange-stained apoptotic bodies; necrotic cells were stained red; and untreated HeLa cells were uniformly green. Significant differences in apoptosis induction were observed between control and fucoidan-treated cancer cells after 24 h, with apoptosis levels notably higher in the treated group.

Figure 7A and **B** illustrate the differential effects of treatment on cell viability and apoptosis. In **Figure 7A**, the majority of the cells exhibit red-to-orange fluorescence, indicating that they are either in the late stages of apoptosis or have undergone necrosis. AO stains all nucleated cells green by binding to DNA, while EB, which can only penetrate cells with compromised membranes, intercalates with DNA and fluoresces red or orange. Therefore, the dominance of red/orange nuclei signifies a high level of membrane permeability and nuclear damage, typical of late apoptotic or necrotic cells. The presence of nuclear condensation and fragmentation further supports this interpretation, suggesting that the cell population has been exposed to a strong apoptotic stimulus, which is the high concentration of fucoidan. **Figure 7B** predominantly shows green fluorescent cells with intact, round nuclei, indicative of healthy or early apoptotic cells. AO can easily penetrate these cells and bind to their DNA, producing green fluorescence, while EB is excluded due to the intact cell membranes. The sparse distribution of orange or red cells suggests that only a small portion of the cells is undergoing apoptosis or necrosis. This result suggests minimal cytotoxic effect due to the absence of fucoidan treatment. These results highlight the apoptosis-inducing properties of fucoidan and visually confirm apoptosis induction, complementing quantitative assays, such as MTT or cell viability curves. Together, these images provide a clear representation of how AO/EB staining can differentiate

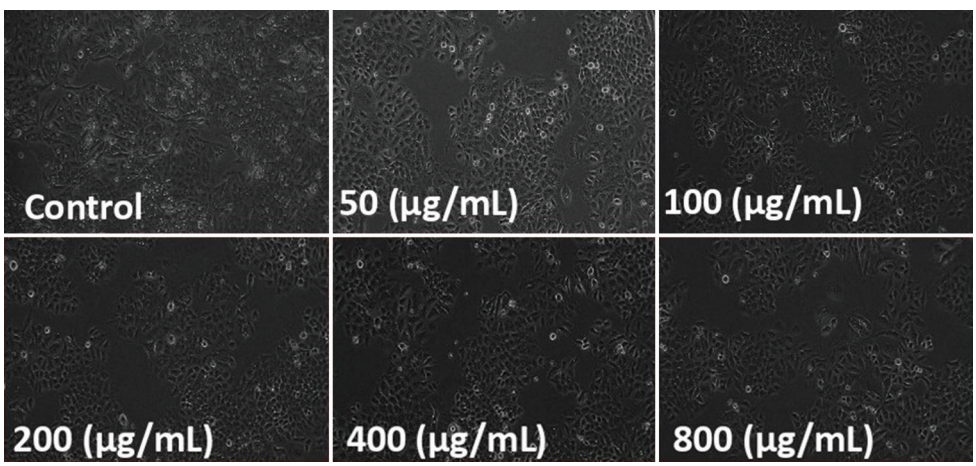

Figure 5. Microscopic images of HeLa (human cervical cancer) cell line treated with different concentrations of fucoidan (0 [Control], 50, 100, 200, 400, 800 µg/mL).

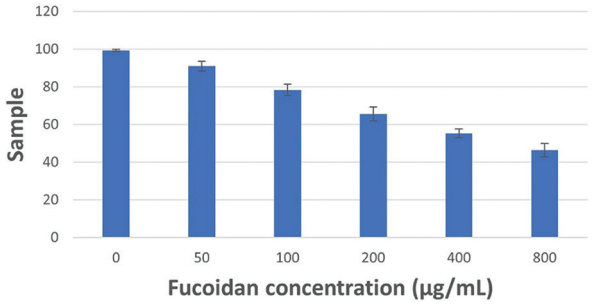

Figure 6. Dose-dependent graph of HeLa (human cervical cancer) cell line treated with different concentrations of fucoidan (0 [Control], 50, 100, 200, 400, 800 µg/mL).

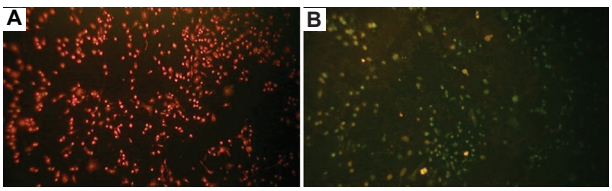

Figure 7. Fluorescence microscopy images of HeLa cells stained with acridine orange and ethidium bromide. (A) Treated with fucoidan: condensed form of nuclei in apoptotic cells and apoptotic bodies were stained orange. (B) Untreated control: condensed form of nuclei in necrotic cells was stained red, and the untreated HeLa cells were stained uniformly green.

between viable, early apoptotic, and late apoptotic/necrotic cells based on membrane integrity and nuclear morphology.

3.6.4. Detection of ROSs using carboxy-2',7'-dichlorodihydrofluorescein diacetate

Bright green fluorescence indicated increased cytosolic ROS generation, a result of oxidative stress, as shown in hydrogen peroxide-treated positive control cells. Reduced green fluorescence indicates lower oxidative stress, as shown in fucoidan-treated cells exhibiting antioxidant properties. The detection of ROS using the carboxy-H_2DCFDA fluorescent probe is a widely used method to evaluate oxidative stress in cells. Carboxy-H_2DCFDA is a cell-permeable, non-fluorescent compound that, upon entering the cell, is deacetylated by intracellular esterases and subsequently oxidized by ROS to form the highly fluorescent compound 2',7'-dichlorofluorescein.

In **Figure 8A**, a strong green fluorescence was observed, indicating elevated ROS produced within the cells. This suggests that the cells are undergoing oxidative stress, possibly induced by a treatment, such as fucoidan. The bright and widespread green fluorescence reflects a high intracellular ROS level, which can lead to oxidative damage, mitochondrial dysfunction, and ultimately cell death if not regulated. Similarly, the control group exhibits little to no green fluorescence, indicating low or negligible ROS levels[39] (**Figure 8B**). The absence of fluorescence suggests that the cellular redox state is balanced and that antioxidant mechanisms are effectively mitigating any ROS generation. Together, these images provide a visual representation of ROS induction, with **Figure 8A** confirming oxidative stress due to external stimuli, while **Figure 8B** serves as a baseline reference for normal ROS activity. The use of

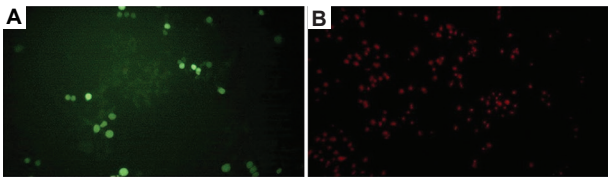

Figure 8. Carboxy-2',7'-dichlorodihydrofluorescein diacetate fluorescent probe images for the detection of reactive oxygen species (ROSs). (A) A strong green fluorescence, indicating elevated ROSs production within the treated cells. (B) Control group with little to no green fluorescence, indicating low or negligible ROS levels.

carboxy-H_2DCFDA thus offers a reliable and sensitive method for detecting oxidative stress in live cells, playing a crucial role in understanding cellular responses to therapeutic agents and environmental challenges.

4. Applications, study limitations, and future directions

Applications of fucoidan extracted from *T. conoides* primarily include nutraceuticals and pharmaceuticals. This is due to its promising dual-action capabilities as an antioxidant and an anticancer agent. Fucoidan has demonstrated strong antioxidant activity, suggesting its potential use as a functional bioactive compound to combat oxidative stress. This positions it as a valuable natural ingredient for promoting general health. The study highlights fucoidan's potential as a therapeutic agent for cancer. It showed a selective, dose-dependent cytotoxic effect on HeLa cervical cancer cells, while having minimal impact on normal L6 cells. This selective toxicity is a highly desirable characteristic for cancer treatments. The mechanism of action involves inducing apoptosis (programmed cell death) and generating ROS in cancer cells, which leads to elevated oxidative stress and ultimately cell death. The research indicates that the fucoidan from *T. conoides* could be developed into a therapeutic compound that targets malignant cells through oxidative stress pathways, while sparing healthy tissue.

A few limitations remain in this study: (i) The process of fucoidan extraction and optimization is still in its early stage, and purification methodologies have not been fully optimized. (ii) Molecular-level studies are limited, hindering the understanding of the in-depth mechanism of action. (iii) The biological study has thus far been restricted to a limited number of cell lines, which does not permit full knowledge of its greater therapeutic scope. In addition, *in vivo* validation in animal models remains limited, thus hindering the translation of results into clinical practice. Filling these lacunae through extensive molecular research, large-scale cell line screening, and well-planned animal studies will be fundamental to further developing the biomedical applications of fucoidan.

5. Conclusions

The present study successfully demonstrates that fucoidan, a sulfated polysaccharide from the brown seaweed *T. conoides*, is a promising dual-action compound. Using the BBD-RSM, the optimized extraction conditions were identified with a buffer-to-algal ratio of 1:40 g/mL, an extraction time of 3 h, a pH of 3, and an extraction temperature of 70°C. Beyond

the optimized extraction, the study's key findings highlight fucoidan's significant antioxidant activity and its potential as an anticancer agent. The research showed that fucoidan exhibits selective cytotoxicity, effectively reducing the viability of HeLa cervical cancer cells in a dose-dependent manner, with minimal impact on normal L6 cells. This selective effect is mediated by the induction of apoptosis (as confirmed by AO/EB double staining) and the generation of ROS, which increases oxidative stress specifically in the cancer cells. The results collectively position fucoidan from *T. conoides* as a valuable natural ingredient for the development of nutraceutical and pharmaceutical applications aimed at promoting human health.

Acknowledgement

The researchers would like to thank the Centre for Environmental and Research Development Unit (Loyola Institute of Frontier Energy), Loyola College, and Environnex Innovation and Research Foundation for their support and assistance throughout the study.

Financial support

None.

Conflicts of interest statement

The authors declare that there is no competing interest.

Author contributions

Conceptualization: SV and PD.; *Formal analysis:* PD and SIK; *Methodology*: PD and SIK; *Funding acquisition:* MKAAR and AM; *Writing – original draft*: PD and SIK; *Writing–review & editing:* MKAAR and AM. All authors have read and agreed to the published version of the manuscript.

Ethics approval and consent to participate

Not applicable.

Consent for publication

Not applicable.

Availability of data

Data are available upon request from the corresponding authors.

Open-access statement

This is an open-access journal, and articles are distributed under the terms of the Creative Commons Attribution-Non-Commercial Share Alike 4.0 License, which allows others to remix, tweak, and build upon the work non-commercially if appropriate credit is given. The new creations are licensed under identical terms.

References

1. Satapathy P, Nazli Khatib M, Neyazi A, *et al.* Prevalence of human papilloma virus among cervical cancer patients in India a systematic review and meta-analysis. *Medcine (Baltimore).* 2024;103(31):e38827. doi: 10.1097/MD.0000000000038827
2. Mathur P, Sathishkumar K, Chaturvedi M, *et al.* Cancer statistics, 2020: Report from national cancer registry programme, India. *JCO Glob Oncol.* 2020;6:1063-1075. doi: 10.1200/go.20.00122.
3. Gupta K, Mandal R, Chatterjee P. Navigating the landscape of cervical cancer in India: Epidemiology, prevention, current status, and emerging solutions. *J Obstet Gynaecol Res.* 2024;50(S1):55-64. doi: 10.1111/jog.16030.
4. Colney Z, Laldinmawii G, Singson S. Unveiling the burden of human papillomavirus infection and risk factors among Indigenous women in Mizoram, Northeast India. *BMC Infect Dis.* 2025;25(1):1406. doi: 10.1186/s12879-025-11529-7
5. Khan A, Kanwal F, Ullah S, *et al.* Plant secondary metabolites-central regulators against abiotic and biotic stresses. *Metabolites.* 2025;15(4):276. doi: 10.3390/metabol5040276
6. Cunha L, Grenha A. Sulfated seaweed polysaccharides as multifunctional materials in drug delivery applications. *Mar Drugs.* 2016;14(3):42. doi: 10.3390/md14030042.
7. Ngo DH, Kim SK. Sulfated polysaccharides as bioactive agents from marine algae. *Int J Biol Macromol.* 2013;62:70-75. doi: 10.1016/j.ijbiomac.2013.08.036
8. Venkatesan J, Lowe B, Anil S, *et al.* Seaweed polysaccharides and their potential biomedical applications. *Starch Stärke.* 2015;67(5-6):381-390. doi: 10.1002/star.201400127.
9. Puvaneswary S, Raghavendran HB, Talebian S, *et al.* Incorporation of fucoidan in β-tricalcium phosphate-chitosan scaffold prompts the differentiation of human bone marrow stromal cells into osteogenic lineage. *Sci Rep.* 2016;6:24202. doi: 10.1038/srep24202.
10. Feng Q, Ma J, Jiang X, *et al.* Therapeutic potential of fucoidan in atherosclerosis: A review. *Food Funct.* 2025;16:4242-4256. doi: 10.1039/D4FO05388E
11. Zhao Y, Limin N, Zhu P, Jiang J, Yao Z, Zhu B. The origin, properties, structure, catalytic mechanism, and applications of fucoidan-degrading enzymes. *Mar Drugs.* 2025;23(3):97. doi: 10.3390/md23030097
12. Rhein-Knudsen N, Reyes-Weiss D, Horn SJ. Extraction of high purity fucoidans from brown seaweeds using cellulases and alginate lyases. *Int J Biol Macromol.* 2023;229:199-209. doi: 10.1016/j.ijbiomac.2022.12.261
13. Wang J, Zhang J, Zhao B, Wang X, Wu Y, Yao J. A comparison study on microwave-assisted extraction of *Potentilla anserina* L. Polysaccharides with conventional method: Molecule weight and antioxidant activities evaluation. *Carbohydr Polym.* 2010;80(1):84-93. doi: 10.1016/j.carbpol.2009.10.073
14. Granato D, De Araújo Calado VM. The use and importance of design of experiments (DOE) in process modelling in food science and technology. In: *Mathematical and Statistical Methods in Food Science and Technology.* United States: John Wiley and Sons, Ltd.; 2013. doi: 10.1002/9781118434635
15. Zhang L, Xu Y, Li Y, Bao T, Gowd V, Chen W. Protective property of mulberry digest against oxidative stress - a potential approach to ameliorate dietary acrylamide-induced cytotoxicity. *Food Chem.* 2017;230:306-315. doi: 10.1016/j.foodchem.2017.03.045
16. Li F, Zhang X, Zheng S, Lu K, Zhao G, Ming J. The composition, antioxidant and antiproliferative capacities of phenolic compounds extracted from tartary buckwheat bran [*Fagopyrum tartaricum* (L.) Gaerth]. *J Funct Foods.* 2016;22:145-155. doi: 10.1016/j.jff.2016.01.027.
17. Dana J, Ravichandran R, Haridas PC, Delfia A, Uchoi D, Chatterjee NS. Insights from untargeted metabolomics and moleuclar networking on the effect of infrared drying and electrical oven drying of *Turbinaria conoides* (J.Agardh) kuzing for nutraceutical application. *Food Hum.* 2025;4:100630. doi: 10.1016/j.foohum.2025.100630
18. Baliyan S, Mukherjee R, Priyadarshini A, *et al.* Determination of antioxidants by DPPH radical scavenging activity and quantitative phytochemical analysis of *Ficus religiosa. Molecules* 2022;27(4):1326. doi: 10.3390/molecules27041326
19. Krishnamurthy M, Selvaraju M, Tamilarasan M. *Turbinaria Conoides* (J. Agardh) sulfated polysaccharide protects rat's heart against myocardial injury. *Int J Biol Macromol.* 2012;50(5):1275-1279. doi: 10.1016/j.ijbiomac.2012.03.012
20. Duan Y, Li J, Jing X, Ding X, Yu Y, Zhao Q. Fucoidan induces apoptosis and inhibits proliferation of hepatocellular carcinoma via the P38 MAPK/ERK and Pi3k/Akt signal pathways. *Cancer Manag Res.* 2020;12:1713-1723. doi: 10.2147/CMAR.S243495
21. Chantree P, Na-Bangchang K, Martviset P. Anticancer activity of fucoidan via apoptosis and cell cycle arrest on cholangiocarcinoma cell. *Asian Pacific J Cancer Prev.* 2021;22(1):209-217. doi: 10.31557/APJCP.2021.22.1.209
22. Cruz Riquelme RT, Colona-Vallejos EH, Alzamora-Gonzales L, Condori Macuri RM. Fucoidan from *Lessonia trabeculata* induces apoptosis through caspase dependent and caspase-independent activation in 4T1 breast adenocarcinoma *in vitro*. *Mar Drugs.* 2024;22(6):251. doi: 10.3390/md22060251
23. Wang G, Guo C, Pi H, *et al.* Elucidation of the anti-colorectal cancer mechanism of *Atractylodes lancea* by network pharmacology and experimental verification. *Aging (Albany NY).* 2024;16(16):12008-12028.

doi: 10.18632/aging.206075

24. Abdollah MRA, Ali AA, Elgohary HH, Elmazar MM. Antiangiogenic drugs in combination with seaweed fucoidan: A mechanistic *in vitro* and *in vivo* study exploring the VEGF receptor and its downstream signaling molecules in hepatic cancer. *Front Pharmacol.* 2023;14:1108992. doi: 10.3389/fphar.2023.1108992
25. Alqathama A. Natural products as promising modulators of breast cancer immunotherapy. *Front Immunol.* 2024;15:1410300. doi: 10.3389/fimmu.2024.1410300
26. Jin JO, Chauhan PS, Arukha AP, Chavda V, Dubey A, Yadav D. The therapeutic potential of the anticancer activity of fucoidan: Current advances and hurdles. *Mar Drugs.* 2021;19(5):265. doi: 10.3390/md19050265
27. Suresh V, Anbazhagan C, Thangam R, *et al.* Stabilization of mitochondrial and microsomal function of fucoidan from sargassum plagiophyllum in diethylnitrosamine induced hepatocarcinogenesis. *Carbohydr Polym.* 2013;92(2):1377-1385. doi: 10.1016/j.carbpol.2012.10.038
28. Chen HY, Chen C. Importance of using modern regression analysis for response surface models in science and technology. *Appl Sci.* 2025;15(13):7206. doi: 10.3390/app15137206
29. Kim S, Asnin L, Assefa AD, Ko EY, Sharma K, Park SW. Extraction of antioxidants from *Aloe vera* Leaf gel: A response surface methodology study. *Food Anal Methods.* 2014;7:1804-1815. doi: 10.1007/s12161-014-9822-x
30. Cui Y, Liu X, Li S, *et al.* Extraction, characterization and biological activity of sulfated polysaccharides from seaweed dictyopteris divaricata. *Int J Biol Macromol.* 2018;117:256-263. doi: 10.1016/j.ijbiomac.2018.05.134
31. Liyana-Pathirana CM, Shahidi F. Antioxidant activity of commercial soft and hard wheat (*Triticum aestivum* L.) as affected by gastric PH conditions. *J Agric Food Chem.* 2005;53(7):2433-2440. doi: 10.1021/jf049320i
32. Mosmann T. Rapid colorimetric assay for cellular growth and survival: Application to proliferation and cytotoxicity assays. *J Immunol Methods.* 1983;65(1-2):55-63. doi: 10.1016/0022-1759(83)90303-4
33. Turczyn R, Krukiewicz K, Katunin A, Sroka J, Sul P. Fabrication and application of electrically conducting composites for electromagnetic interference shielding of remotely piloted aircraft systems. *Compos Struct.* 2020;232:111498. doi: 10.1016/j.compstruct.2019.111498
34. Berezhnaya YD, Kazachenko AS, Kazachenko AS, Malyar YN, Borovkova VS. Sulfation of various polysaccharide structures: Different methods and perspectives. *Chem.* 2024;6(4):640-665. doi: 10.3390/chemistry6040038
35. Niyonizigiye I, Ngabire D, Patil MP, Singh AA, Kim G. Do *in vitro* induction of endoplasmic reticulum stress in human cervical adenocarcinoma hela cells by fucoidan. *Int J Biol Macromol.* 2019;137:844-852. doi: 10.1016/j.ijbiomac.2019.07.043
36. Synytsya A, Kim WJ, Kim SM, *et al.* Structure and antitumour activity of fucoidan isolated from sporophyll of Korean brown seaweed undaria pinnatifida. *Carbohydr Polym.* 2010;81(1):41-48. doi: 10.1016/j.carbpol.2010.01.052
37. You SG, Yang C, Lee HY, Lee BY. Molecular characteristics of partially hydrolyzed fucoidans from sporophyll of *Undaria pinnatifida* and their *in vitro* anticancer activity. *Food Chem.* 2010;119(2):554-559. doi: 10.1016/j.foodchem.2009.06.054
38. Ishak RAH, Mortada ND, Zaki NM, El-Shamy AEHA, Awad GAS. Impact of microparticle formulation approaches on drug burst release: A level A IVIVC. *J Microencapsul.* 2014;31(7):674-684. doi: 10.3109/02652048.2014.913724
39. Simon HU, Haj-Yehia A, Levi-Schaffer F. Role of reactive oxygen species (ROS) in apoptosis induction. *Apoptosis.* 2000;5:415-418. doi: 10.1023/A:1009616228304

Received: June 27, 2025
Revised: August 26, 2025
Accepted: October 15, 2025
Available online: November 27, 2025